frontiers | Frontiers in Materials

PERSPECTIVE
published: 01 July 2022
doi: 10.3389/fmats.2022.850115

Synthesis and Characterisation of Mg^{2+} and Al^{3+} Co-Doped $CoCr_2O_4$ Inorganic Pigments With High Near-Infrared Reflectance

Xueling Wei[1], Xiangyu Zou[1], Zhifeng Deng[1], Weiwei Bao[1], Taotao Ai[1] and Qi Zhang[2]**

[1]School of Materials Science and Engineering, Shaanxi University of Technology (SNUT), Hanzhong, China, [2]School of Environmental and Chemistry Engineering, Kunming Metallurgy College, Kunming, China

A new class of near-infrared (NIR) reflectance pigments based on $Co_{1-x}Mg_xCr_{2-y}Al_yO_4$ (x = 0–1 and y = 0–2) was synthesised using the Pechini-type sol-gel process. The developed powders were characterised by thermogravimetry and differential scanning calorimetry, X-ray diffraction (XRD), ultraviolet–visible near-infrared diffuse reflectance spectroscopy, and colour Commission Internationale del'Eclairage (CIE) 1976 (L*a*b*) colour scales. The XRD patterns revealed characteristic peaks of the spinel structure with good crystallinity. Substituting Mg^{2+} for Co^{2+} ions in the tetrahedral positions and Al^{3+} for Cr^{3+} ions in the octahedral positions of $CoCr_2O_4$ reduces the cost and changes the colour of the pigment (green to yellow and then blue). Moreover, the synthesised pigments exhibited high NIR solar reflectance in the 780–2,500 nm wavelength range. The thermal and chemical stability of the pigments was also studied. Our findings demonstrate the potential for applying these pigments in cool colourants.

Keywords: near-infrared reflectance, sol-gel method, Mg^{2+} and Al $^{3+}$ co-doped, cool pigments, solar reflectance

OPEN ACCESS

Edited by:
Weihua Li,
University of Wollongong, Australia

Reviewed by:
Ayman Awad Ali,
Benha University, Egypt

****Correspondence:***
Weiwei Bao
baowei1834@163.com
Qi Zhang
480807767@qq.com

Specialty section:
This article was submitted to Smart Materials, a section of the journal Frontiers in Materials

Received: *07 January 2022*
Accepted: *24 May 2022*
Published: *01 July 2022*

Citation:
Wei X, Zou X, Deng Z, Bao W, Ai T and Zhang Q (2022) Synthesis and Characterisation of Mg^{2+} and Al^{3+} Co-Doped $CoCr_2O_4$ Inorganic Pigments With High Near-Infrared Reflectance. Front. Mater. 9:850115. doi: 10.3389/fmats.2022.850115

HIGHLIGHTS

(1) A new class of near-infrared reflectance pigments based on $Co_{1-x}Mg_xCr_{2-y}Al_yO_4$ (x=0-1 and y=0-2) were synthesised via Pechini-type sol-gel method.
(2) The colours of the pigment samples can be tuned from green to yellow and then blue.
(3) Decreasing the Co and Cr contents reduces the cost and environmental damages.
(4) Pigment properties make it a potential candidate for use as cool pigments.

INTRODUCTION

In recent years, near-infrared (NIR) reflective pigments have received considerable attention in construction, plastic, ink, and military industries. NIR reflective pigments are complex metal oxides with high reflectance for NIR radiation (Song et al., 2019; Ali et al., 2018; Rossi et al., 2020; Jing et al., 2018; Zhou et al., 2020). The everyday use of solar reflective roofing materials has been proven to save energy, alleviate urban heat islands, and curb global warming (Ferrari et al., 2015; Zou and Zhang, 2020; Yang et al., 2017). Most of the literature on NIR reflective pigments are available as patents (Swiler et al., 2003; Blonski et al., 2001), demonstrating their vast applications. Many of these inorganic pigments consist of hazardous heavy metals such as cobalt (Co), lead (Pb), cadmium (Cd),

and chromium (Cr), which are restricted under present environmental regulations. Several of these methods are expensive (Hedayati et al., 2015; Schildhammer et al., 2017; Yuan et al., 2018). Recently, many rare-earth-based NIR reflective pigments have been suggested as substitutes for traditional pigments, owing to their low toxicity (Raj et al., 2019; Han et al., 2014). Aju Thara et al. (2017); Zhao et al. (2015) prepared a series of NIR pigments based on yttrium molybdate ($Y_2Mo_3O_{12}$) and yttrium cerate, and illustrated the NIR reflectance and colouring mechanism. However, rare-earth compounds are expensive because they are difficult to mine.

Numerous methods have been employed to synthesise simple oxide or oxide-based systems. Most conventional methods involve solid-state reactions (Zhang et al., 2018), co-precipitation (Frolova et al., 2017), hydrothermal (McMahon et al., 2019; Elakkiya and Sumathi, 2020), evaporative drying (Droguet et al., 2021), and sol-gel (polymeric precursor method) (Lima et al., 2020). The sol-gel method should be emphasised as it has numerous desirable characteristics, such as using affordable reagents and reducing costs, and requiring low temperature for oxide synthesis. In addition, the method has excellent chemical homogeneity at the molecular level of all components and has easy stoichiometric control in complex systems (Gonzaga et al., 2020).

Spinel pigments, which are represented chemically as AB_2O_4, have generated an increasing interest. These pigments exhibit a myriad of colours and tonalities owing to their ability to accommodate different cations (Bao et al., 2016). For example, cobalt chromite ($CoCr_2O_4$) is an essential commercial material and is extensively used as a catalyst, magnetic compound, and pigment owing to its superior properties. Because cobalt and chromium are generally rare and harmful, incorporating less toxic and expensive metals into the $CoCr_2O_4$ minimises the cost of production and impact on the environment. Therefore, in this study, Mg^{2+} substitution for Co^{2+} and Al^{3+} substitution for Cr^{3+} in $CoCr_2O_4$ was facilitated using the Pechini-type sol-gel process. The effects of these enrichments on the crystal structures, optical properties, and thermal and chemical stabilities of as-synthesised pigments were thoroughly investigated.

EXPERIMENTAL

Materials and Methods

Magnesium nitrate ($Mg(NO_3)_2{\cdot}6H_2O$), cobalt nitrate ($Co(NO_3)_2{\cdot}6H_2O$), citric acid (CA, $C_6H_8O_7$), chromium nitrate ($Cr(NO_3)_3{\cdot}9H_2O$), aluminium nitrate ($Al(NO_3)_3{\cdot}9H_2O$), and ethylene glycol (EG, $C_2H_6O_2$) were the starting materials. All chemicals utilised were analytical grade, acquired from Beijing Chemical Reagent Corporation, and used as received without further purification. All pigment samples of $Co_{1-x}Mg_xCr_{2-y}Al_yO_4$ (x = 0–1 and y = 0–2) were synthesised using the Pechini-type sol-gel method.

First, CA was dissolved in distilled water and stirred continuously at 80°C. Subsequently, nitrates of cobalt, chromium, magnesium, and aluminium were added stoichiometrically into the acid solution. The molar ratio of the CA/metal was 3:1. After dissolution, EG was added at a CA/EG ratio of 3:2. All solutions were mixed using a magnetic stirrer. The resultant solution was then heated on a hot plate at approximately 80°C for approximately 1 h to produce polymerisation gel through a polymerisation reaction. Subsequently, the beaker was kept in a thermostat drier at 120°C for 12 h. The preliminary heat treatment (350°C) of the gel was performed in air for 2 h. Gas liberation by combustion during heat treatment partially degraded the organic structure and its expansion, forming a brittle black powder precursor. Finally, the obtained powder of the precursor was ground into a fine powder and then calcined at 900°C at a heating rate of 10°C/min for 6 h to remove residual organic materials, and powder samples were synthesised.

Characterisation Techniques

Thermogravimetry and differential scanning calorimetry (TG-DSC) were performed using a STAR E TGA/DSC1 instrument to analyse the powder precursor and synthesised pigments. The powdered samples were heated under nitrogen in the temperature range 50–900°C at a rate of 20°C/min. Approximately 10 mg of the sample was loaded into aluminium crucibles for testing. Tabular α-Al_2O_3 was used as the reference for weight loss.

A Rigaku Ultima IV X-ray diffractometer equipped with Ni-filtered Cu Kα radiation (λ = 0.15406 nm, 40 kV, and 40 mA) was used to examine the crystal structures of the synthesised samples at 25°C. Step scanning over an angular range of 2θ (10°–80°) with a step size of 0.02°and a counting time of 5 s at each step were used for data collection.

The diffuse reflectance of the samples was measured with a 5-nm step size in the range 380–2,500 nm using a Lambda 950 UV–vis NIR spectrophotometer with an integrating sphere attachment, calibrated by a white standard (D65 illumination such as daylight).

The colour Commission Internationale del'Eclairage chromaticity analysis software (Perkin Elmer) was used to estimate the pigment colour parameters from the reflection data of visible light. The CIE 1976 L*a*b*colourimetry method was employed following the recommendations of the CIE. In this system, the L* value signifies the lightness or darkness of the colour (L* is equal to 0 and 100 for black and white, respectively). The values of a* (green (−) → red (+) axis) and b* (blue (−) → yellow (+) axis) indicate the colour hue. The parameter C* (chroma) represents the colour saturation and is defined in **Eq. (1)** (Sukmarani et al., 2020; Gong et al., 2021).

$$C^* = \left(a^{*2} + b^{*2}\right)^{1/2}, \tag{1}$$

The measurement standard JG/T 235-2014 was used to guide the calculations for the NIR solar reflectance (R^*) in the wavelength range 780–2,500 nm. The function R^* was determined using **Eq. (2)**, as follows:

$$R^* = \frac{\int_{780}^{2500} r(\lambda) i(\lambda) d(\lambda)}{\int_{780}^{2500} i(\lambda) d(\lambda)}, \tag{2}$$

where $i(\lambda)$ is the solar special irradiance (W m^{-2} nm^{-1}), and $r(\lambda)$ corresponds to the spectral reflectance achieved experimentally

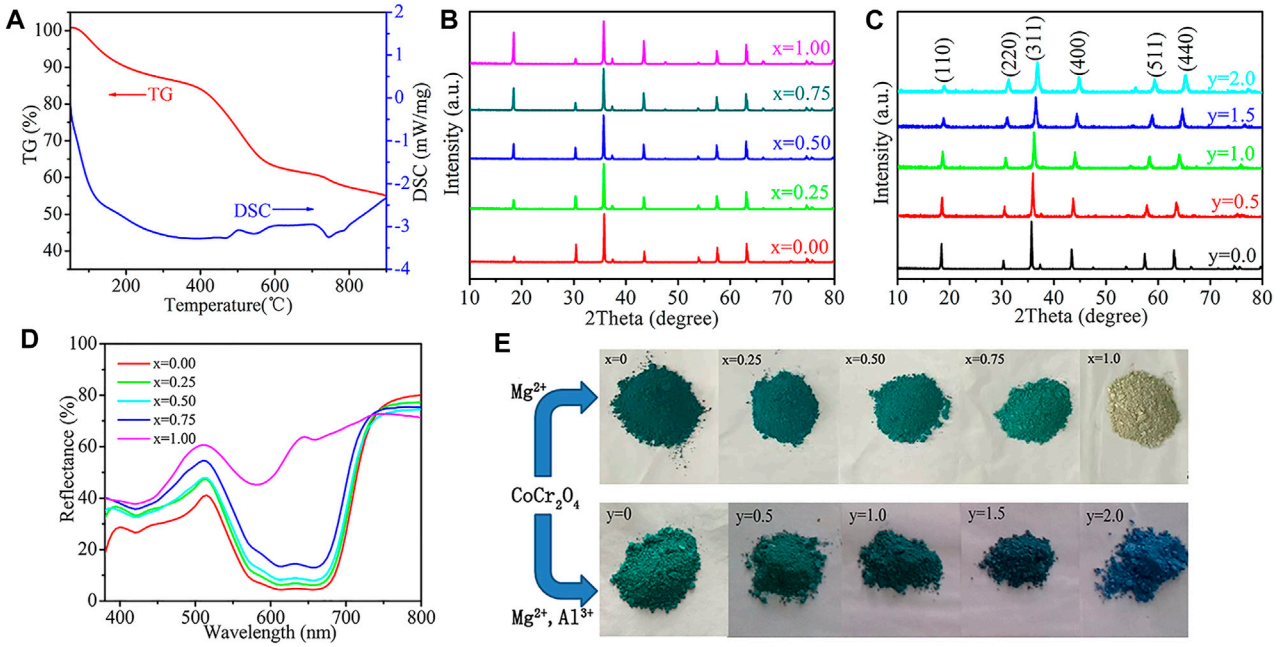

FIGURE 1 | (A) TG-DSC curves of $CoCr_2O_4$ pigment precursor **(B)** XRD diffraction patterns of $Co_{1-x}Mg_xCr_2O_4$ (x = 0.00, 0.25, 0.50, 0.75, 1.00) pigments **(C)** XRD diffraction patterns of $Co_{0.25}Mg_{0.75}Cr_{2-y}Al_yO_4$ (y = 0.0, 0.5, 1.0, 1.5, 2.0) pigments **(D)** UV–vis absorption spectra of $Co_{1-x}Mg_xCr_2O_4$ (x = 0.00, 0.25, 0.50, 0.75, 1.00) powdered pigments **(E)**photographs of $Co_{1-x}Mg_xCr_2O_4$ (x = 0.00–1.00) and $Co_{0.25}Mg_{0.75}Cr_{2-y}Al_yO_4$ (y = 0.0–2.0) pigments.

(W m^{-2}). The NIR solar reflectance value quantifies the unabsorbed solar radiation on the surface of a substance and signifies the build-up of heat in structures upon exposure to the Sun (Hedayati et al., 2015).

RESULTS AND DISCUSSION

Thermal Analysis

Figure 1A shows the thermal analysis (TG-DSC) results for the synthesised pigment. The TG curve depicts three different stages with a total weight loss of 43%, which can be observed from the TG curve. For instance, increasing the temperature (50°C–300°C), decreased the weight of the $CoCr_2O_4$ precursor by 13%. Weight loss is associated with the removal of residual water, unpolymerised CA, and EG from the precursor. The weight loss increased by more than 25% at 300°C–600°C.

An exothermic peak in the DSC curve was observed at approximately 500°C–600°C, indicating the evolution of H_2O, CO_x, and NO_x via the combustion of the nitrates and organic impurities (Liu et al., 2015). Furthermore, a highly exothermic peak in the DSC curve was observed at 700°C–800°C, which was attributed to the precursor decomposition into $CoCr_2O_4$ particles. The mass loss was less than 5% at temperatures higher than 600°C, implying the realisation of final $CoCr_2O_4$ pigments.

Powder X-Ray Diffraction Analysis

Figure 1B shows the XRD patterns of the as-synthesised $Co_{1-x}Mg_xCr_2O_4$ (x = 0.00, 0.25, 0.50, 0.75, and 1.00) precursors after grinding and calcining at 900°C for 6 h. The analysis revealed peaks of the cubic spinel structure, which were observed for all samples. The space groups, Fd3m, of $CoCr_2O_4$ and $MgCr_2O_4$ were distinguished based on JCPDS 22-1084 and 65-3106, respectively. In addition, the XRD patterns did not exhibit non-spinel impurity phases.

Figure 1C illustrates the XRD patterns of $Co_{0.25}Mg_{0.75}Cr_{2-y}Al_yO_4$ (y = 0.0, 0.5, 1.0, 1.5, and 2.0). All the diffraction peaks were associated with the cubic spinel crystal structure of $CoCr_2O_4$, and the structure was not altered by co-doping with Mg^{2+} and Al^{3+}. The addition of Al^{3+} ions slightly shifted the XRD peaks towards higher diffraction angles than the parent oxide. A variation in the cell volume may have caused the observed 2θ shift. Typically, an increase in the Al^{3+} concentration decreases the cell volume because a smaller Al^{3+} (0.051 nm) displaces the larger Cr^{3+} (0.061 nm) ions (Liu et al., 2015; Wu et al., 2018). **Supplementary Tables S1, S2** show that there is no obvious change in cell volume with the increase in Mg concentration in $CoCr_2O_4$, which is mainly due to the similar ionic radii of Mg^{2+} and Co^{2+}. With the increase in Al concentration, the cell volume decreases regularly, indicating that the replacement of Cr by Al is successful. The pigment morphology was characterised by SEM (**Supplementary Figure S1**), and the average grain size was less than 5 μm. Elemental mapping analysis (**Supplementary Figure S2**) further revealed that Cr, Co, O, Mg, and Al elements exhibited a uniform distribution.

Optical Properties of Magnesium Doping

Figure 1D demonstrates the UV–vis absorption spectra of the powdered $Co_{1-x}Mg_xCr_2O_4$ (x = 0.00, 0.25, 0.50, 0.75, and 1.00)

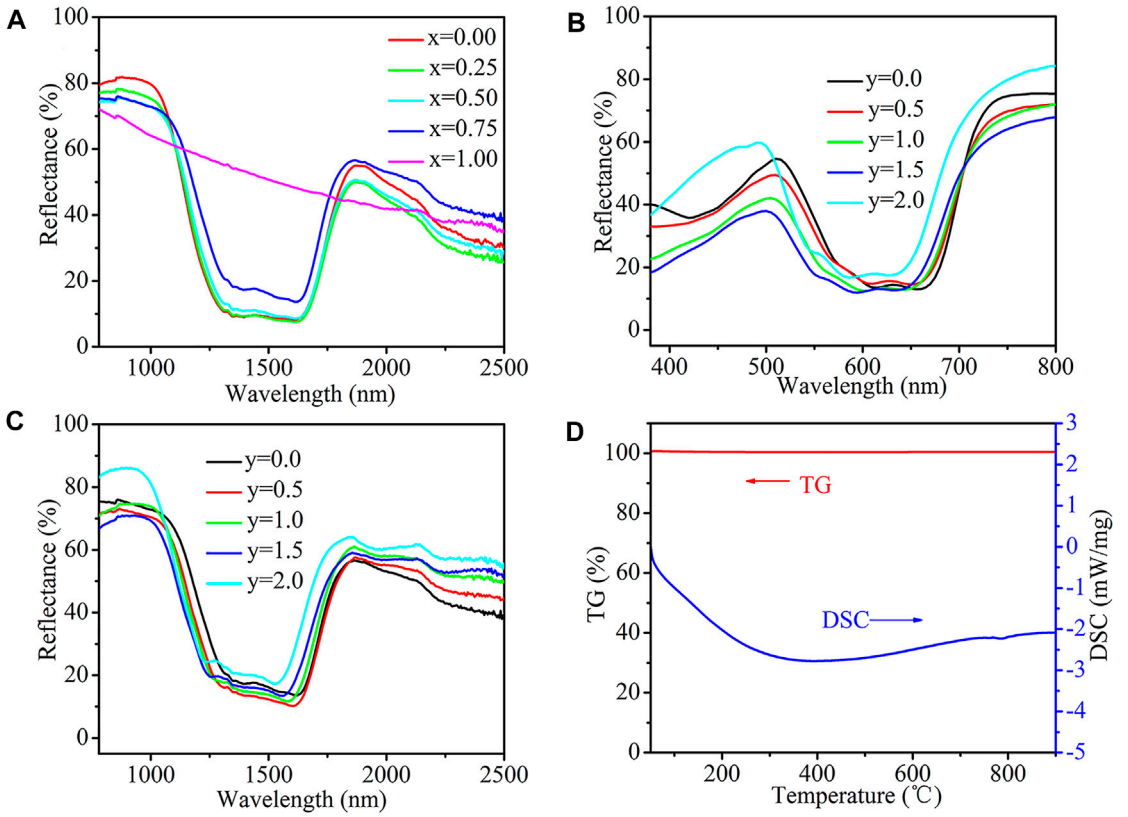

FIGURE 2 | (A) NIR reflectance of $Co_{1-x}Mg_xCr_2O_4$ (x = 0.00, 0.25, 0.50, 0.75, 1.00) powdered samples **(B)** UV–vis absorption spectra of $Co_{0.25}Mg_{0.75}Cr_{2-y}Al_yO_4$ (y = 0.0, 0.5, 1.0, 1.5, 2.0) powdered pigments **(C)** NIR reflectance of $Co_{0.25}Mg_{0.75}Cr_{2-y}Al_yO_4$ (y = 0.0, 0.5, 1.0, 1.5, 2.0) powdered samples **(D)**TG-DSC analysis of powdered $Co_{0.25}Mg_{0.75}Al_2O_4$ pigment sample.

samples. An intense triple band at approximately 570, 610, and 660 nm was observed for the $CoCr_2O_4$ sample spectrum. The absorption peaks steadily weakened with increasing and decreasing concentrations of Mg and Co, respectively. According to the Tanabe–Sugano energy level diagrams, the ^4F ground-state term separates into three terms, $^4A_2$, $^4T_2$, and $^4T_1(F)$ in the tetrahedral coordination of Co^{2+} ions with the d^7 configuration, while the ^4P excited-state term transforms into $^4T_1(P)$. Thus, the three possible spin transitions are ν_1: $^4A_2(F) \rightarrow {}^4T_2(F)$, ν_2: $^4A_2(F) \rightarrow {}^4T_1(F)$, and ν_3: $^4A_2(F) \rightarrow {}^4T_1(P)$. The first and second bands lie within the IR region, whereas the third band lies in the visible region. The broadband can be ascribed to the ν_3 transition ($^4A_2(F) \rightarrow {}^4T_1(P)$ transition) of Co^{2+} ions, which decomposes into three bands because of L-S Russell–Saunders coupling (Hedayati et al., 2015; Lourenco et al., 2016). Therefore, this broad triple band within 500 and 700 nm results in blue pigmentation of compounds containing Co^{2+}.

The chromatic properties of the synthesised $Co_{1-x}Mg_xCr_2O_4$ pigments were assessed using their CIE 1976 L*a*b*colour coordinates (**Supplementary Table S3**). The addition of Mg^{2+} lightened the colour of the samples, as evidenced by the increasing L* from 52.92 to 77.56. In contrast, increasing Mg^{2+} substitution results in the loss of the green pigment hue, as is apparent from the change in the colour coordinate a* from −38.80 to −7.32. Moreover, the b* values increased from −15.43 to 9.14, indicating intensification of the yellow colour in the pigments. The C* values, representing the richness of the colour hue, decreased significantly from 41.76 to 11.71. The observed hue angles of the pigments are found to be in the green region of the cylindrical colour space. **Figure 1E** shows the photographs of the synthesised powdered pigment samples.

Figure 2A shows the NIR reflectance spectra of the $Co_{1-x}Mg_xCr_2O_4$ pigments. The base compound, $CoCr_2O_4$, has an NIR solar reflectance (R*) of 55.1%. Simultaneously, substituting Co^{2+} ions with Mg^{2+} ions decreased the NIR reflectance of the pigments from 55.1 (x = 0.00) to 52.8% (x = 0.50). Further doping of Mg^{2+} with Co^{2+} increased the NIR reflectance to 60.3% (x = 1.00). **Supplementary Table S3** presents detailed information on the NIR solar reflectance of the powdered pigments. The NIR reflectance of a typical pigment sample $Co_{0.25}Mg_{0.75}Cr_2O_4$ (R* = 56.3%) was significantly higher than that of the Y_2BaCuO_5 green pigment reported elsewhere (R* = 50%) (Shankland et al., 1974; Jose et al., 2014). The designed class of pigments displayed high reflectance in the NIR region, suggesting that these formulations could be considered cooling pigments. In addition, with the increase in Mg doping amount, the as-prepared pigments showed a red shift in the band gap transition.

Optical Properties of Aluminium Doping

Figure 2B illustrates the UV–vis absorption spectra of the developed $Co_{0.25}Mg_{0.75}Cr_{2-y}Al_yO_4$ (y = 0.0, 0.5, 1.0, 1.5, and 2.0) samples. A prominent blue shift of the triple band occurred when the Al^{3+} content was increased from 0 to 2. The energy level of the excitation state for Co^{2+} and the position of the absorption band are dependent on the Co^{2+} ion surroundings. The gradual substitution of Al^{3+} for Cr^{3+} indicates a substantial change in the volume of the octahedral site. Subsequently, oxygen ligands experience less attraction from octahedrally coordinated ions because of the lower atomic mass of aluminium than that of chromium. Therefore, the exposure of the oxygen ligands is more to $Mg^{2+}$and Co^{2+}, enhancing the splitting of the d-orbital energy levels and the blue shift of the absorption band (**Figure 2B**) (Hedayati et al., 2015; Shankland et al., 1974).

The chromatic properties of the synthesised $Co_{0.25}Mg_{0.75}Cr_{2-y}Al_yO_4$ pigments were obtained from their CIE 1976 L*a*b* colour coordinates (**Supplementary Table S4**). Substituting Al^{3+} for Cr^{3+} in $Co_{0.25}Mg_{0.75}Cr_2O_4$ spinel increased a* and decreased b*, weakening the intensity of the green colour in the pigments while enhancing the blue pigmentation. Substituting Al^{3+} with Cr^{3+} ions in the spinel structure decreased L* from 64.82 to 53.87, darkening the samples. Consequently, C*, which represents the richness of the colour hue, decreased from 34.93 to 24.33. However, the L* and C* values changed slightly when Al^{3+} was completely substituted with Cr^{3+} ions in the spinel structure. With the increasement of Al doping, the hue angles of pigment move from green to blue region of the cylindrical colour space. **Figure 1E** shows photographs of the synthesised powdered pigment samples.

Figure 2C shows the NIR reflectance spectra of the powdered samples. The NIR solar reflectance of the samples decreased from 56.3 (y = 0.0) to 51.9 (y = 1.5) with the substitution of Al^{3+} for Cr^{3+}. **Supplementary Table S4** lists the NIR solar reflectance of the powdered pigments. The reflectance reached a maximum (R* = 61.7%) for y = 2.0, which was higher than that of aluminium-doped cobalt chromite pigments of similar colour, as reported elsewhere (R* = 52%) (Hedayati et al., 2015). Furthermore, with the increase in Al doping amount, the as-obtained pigments also exhibit a red shift in the band gap transition. These observations demonstrate that Mg^{2+} and Al^{3+} co-doped $CoCr_2O_4$ systems are appropriate cooling pigments.

Studies on Thermal and Chemical Stabilities of the Pigments

The $Co_{0.25}Mg_{0.75}Al_2O_4$ pigments were investigated from 50 to 900 °C for their thermal stability. The results indicated that there was a negligible weight loss and phase transition of the pigment (**Figure 2D**). The chemical resistance of the pigment was investigated using 5% $HCl/H_2SO_4/HNO_3$ and NaOH (Bao et al., 2016; Jose and Reddy, 2013). A pre-weighed pigment powder was soaked in an acid/alkali solution for 30 min and stirred using a magnetic stirrer. The pigment powder slurry was filtered, washed with water, dried, and weighed again. Negligible weight loss of the pigment was observed for all the tested acids and alkalis. The colour coordinates of the pigments were measured and had negligible total colour difference (△E*) (**Supplementary Table S5**). These results demonstrate that the pigments were chemically and thermally stable.

CONCLUSION

In this study, a series of NIR reflective pigments with the general formula $Co_{1-x}Mg_xCr_{2-y}Al_yO_4$ (x = 0–1 and y = 0–2) were synthesised using the Pechini-type sol-gel method. The effect of Mg^{2+} and Al^{3+} enrichment on the structure and optical and chromatic properties of the products was investigated. XRD analyses revealed that the pigments were well crystallised in spinel cubic structures. The pigments exhibited a wide range of colours from green to yellow and blue and showed clear NIR reflective performance (greater than 51%). The pigments also showed good thermal and chemical stability.

DATA AVAILABILITY STATEMENT

The original contributions presented in the study are included in the article/**Supplementary Material**, and further inquiries can be directed to the corresponding authors.

AUTHOR CONTRIBUTIONS

XW and XZ: Synthesis of pigments and corresponding characterisations and analysis; writing of original drafts. DZ and TA: helped in data analysis; WB revised the manuscript.

FUNDING

This research was supported by the National Natural Science Foundation of China (Grant Nos. 51504147) and the National & Local Joint Engineering Laboratory for Slag Comprehensive Utilization and Environmental Technology Open Fund (Grant Nos. SLGPT2019KF01-03).

SUPPLEMENTARY MATERIAL

The Supplementary Material for this article can be found online at: https://www.frontiersin.org/articles/10.3389/fmats.2022.850115/full#supplementary-material

REFERENCES

Aju Thara, T. R., Rao, P. P., Divya, S., Raj, A. K. V., and Sreena, T. S. (2017). Enhanced Near Infrared Reflectance with Brilliant Yellow Hues in Scheelite Type Solid Solutions, $(LiLaZn)_{1/3}MoO_4$-$BiVO_4$ for Energy Saving Products. *ACS Sustain. Chem. Eng.* 5, 5118–5126. doi:10.1021/acssuschemeng.7b00485

Ali, A. A., El Fadaly, E., and Ahmed, I. S. (2018). Near-infrared Reflecting Blue Inorganic Nano-Pigment Based on Cobalt Aluminate Spinel *via* Combustion Synthesis Method. *Dyes Pigments* 158, 451–462. doi:10.1016/j.dyepig.2018.05.058

Bao, W., Ma, F., Zhang, Y., Hao, X., Deng, Z., Zou, X., et al. (2016). Synthesis and Characterization of Fe^{3+} Doped $Co_{0.5}Mg_{0.5}Al_2O_4$ Inorganic Pigments with High Near-Infrared Reflectance. *Powder Technol.* 292, 7–13. doi:10.1016/j.powtec.2016.01.013

Blonski, R. P., Pipoly, R. A., and Sliwinski, T. R. (2001). *Infrared Reflective Color Pigment*. EP1141105 A1.

Droguet, B., Liang, H., Frka-Petesic, B., Parker, R., De Volder, M., Baumberg, J., et al. (2021). Large-scale Fabrication of Structurally Coloured Cellulose Nanocrystal Films and Effect Pigments. *Nat. Mater.* 21, 352–358.doi:10.1038/s41563-021-01135-8

Elakkiya, V., and Sumathi, S. (2020). Low-temperature Synthesis of Environment-Friendly Cool Yellow Pigment: Ce Substituted $SrMoO_4$. *Mater. Lett.* 263, 127246. doi:10.1016/j.matlet.2019.1272460167

Ferrari, C., Muscio, A., Siligardi, C., and Manfredini, T. (2015). Design of a Cool Color Glaze for Solar Reflective Tile Application. *Ceram. Int.* 41, 11106–11116. doi:10.1016/j.ceramint.2015.05.058

Frolova, L., Pivovarov, A., and Butyrina, T. (2017). Synthesis of Pigments in Fe_2O_3-Al_2O_3-CoO by Co-precipitation Method. *Prt* 46, 356–361. doi:10.1108/PRT-07-2016-0073

Gong, L., Liang, J., Kong, L., Chen, B., Li, Y., and Tian, G. (2021). Synthesis of High-Performance Copper Barium Silicate Composite Pigment from Waste Iron Ore Tailings. *Ceram. Int.* 47, 27987–27997. doi:10.1016/j.ceramint.2021.06.230

Gonzaga, L. A., Santana, V. T., Bernardi, M. I. B., Hrubý, J., Neugebauer, P., and Mesquita, A. (2020). CeO_2 and CeO_2 :Pr Nanocrystalline Powders Prepared by the Polymeric Precursor Method: Yellow and Red Pigments with Tunable Color. *J. Am. Ceram. Soc.* 103, 6280–6288. doi:10.1111/jace.17339

Han, A., Ye, M., Liu, L., Feng, W., and Zhao, M. (2014). Estimating Thermal Performance of Cool Coatings Colored with High Near-Infrared Reflective Inorganic Pigments: Iron Doped $La_2Mo_2O_7$ Compounds. *Energy Build.* 84, 698–703. doi:10.1016/j.enbuild.2014.08.024

Hedayati, H. R., Sabbagh Alvani, A. A., Sameie, H., Salimi, R., Moosakhani, S., Tabatabaee, F., et al. (2015). Synthesis and Characterization of $Co_{1-x}Zn_xCr_{2-y}Al_yO_4$ as a Near-Infrared Reflective Color Tunable Nano-Pigment. *Dyes Pigments* 113, 588–595. doi:10.1016/j.dyepig.2014.09.030

Jing, J., Zhang, Y., Sun, J., Zhao, X., Gao, D., and Zhang, Y. (2018). A Comparative Study on Different RE-doped (RE=Pr, Nd, Sm) $SrCuSi_4O_{10}$ Blue Pigments with High Near-Infrared Reflectance. *Dyes Pigments* 150, 9–15. doi:10.1016/j.dyepig.2017.10.045

Jose, S., Prakash, A., Laha, S., and Natarajan, S. (2014). Green Colored Nano-Pigments Derived from Y_2BaCuO_5: NIR Reflective Coatings. *Dyes Pigments* 107, 118–126. doi:10.1016/j.dyepig.2014.03.025

Jose, S., and Reddy, M. L. (2013). Lanthanum-strontium Copper Silicates as Intense Blue Inorganic Pigments with High Near-Infrared Reflectance. *Dyes Pigments* 98, 540–546. doi:10.1016/j.dyepig.2013.04.013

Lima, N. A., Alencar, L. D. S., Siu-Li, M., Feitosa, C. A. C., Mesquita, A., M'peko, J.-C., et al. (2020). $NiWO_4$ Powders Prepared via Polymeric Precursor Method for Application as Ceramic Luminescent Pigments. *J. Adv. Ceram.* 9, 55–63. doi:10.1007/s40145-019-0347-z

Liu, L., Han, A., Ye, M., and Zhao, M. (2015). Synthesis and Characterization of Al^{3+} Doped $LaFeO_3$ Compounds: A Novel Inorganic Pigments with High Near-Infrared Reflectance. *Sol. Energy Mater. Sol. Cells* 132, 377–384. doi:10.1016/j.solmat.2014.08.048

Lourenço, S. A., Silva, R. S., and Dantas, N. O. (2016). Tunable Dual Emission in Visible and Near-Infrared Spectra Using Co^{2+}-Doped PbSe Nanocrystals Embedded in a Chalcogenide Glass Matrix. *Phys. Chem. Chem. Phys.* 18, 23036–23043. doi:10.1039/c6cp04419k

McMahon, M. E., Santucci, R. J., Glover, C. F., Kannan, B., Walsh, Z. R., and Scully, J. R. (2019). A Review of Modern Assessment Methods for Metal and Metal-Oxide Based Primers for Substrate Corrosion Protection. *Front. Mat.* 6, 190–213. doi:10.3389/fmats.2019.00190

Raj, A. K. V., Rao, P. P., Sreena, T. S., and Thara, T. R. A. (2019). Pigmentary Colors from Yellow to Red in $Bi_2Ce_2O_7$ by Rare Earth Ion Substitutions as Possible High NIR Reflecting Pigments. *Dyes Pigments* 160, 177–187. doi:10.1016/j.dyepig.2018.08.010

Rossi, S., Lindmark, H., and Fedel, M. (2020). Colored Paints Containing NIR-Reflective Pigments Exposed to Accelerated Ultraviolet Radiation Aging with Possible Application as Roof Coatings. *Coatings* 10, 1135–1152. doi:10.3390/coatings10111135

Schildhammer, D., Fuhrmann, G., Petschnig, L., Schottenberger, H., and Huppertz, H. (2017). Synthesis and Optical Properties of New Highly NIR Reflective Inorganic Pigments $RE_6Mo_2O_{15}$ (RE = Tb, Dy, Ho, Er). *Dyes Pigments* 140, 22–28. doi:10.1016/j.dyepig.2017.01.021

Shankland, T. J., Duba, A. G., and Woronow, A. (1974). Pressure Shifts of Optical Absorption Bands in Iron-Bearing Garnet, Spinel, Olivine, Pyroxene, and Periclase. *J. Geophys. Res.* 79, 3273–3282. doi:10.1029/jb079i023p03273

Song, Y., Chen, W., Lim, X. M., Hu, X., Liu, M., and Zhang, Q. (2019). Electronic Configuration in Outset Orbitals of Doping Elements Plays as a Key Factor in Tuning Near Infrared Reflection of $YMn_{0.9}M_{0.1}O_3$ (M = Cr, Mn, Fe, Co, Al, Ga and In). *J. Solid State Chem.* 273, 81–84. doi:10.1016/j.jssc.2019.02.040

Sukmarani, G., Kusumaningrum, R., Noviyanto, A., Fauzi, F., Habieb, A. M., Amal, M. I., et al. (2020). Synthesis of Manganese Ferrite from Manganese Ore Prepared by Mechanical Milling and its Application as an Inorganic Heat-Resistant Pigment. *J. Mater. Res. Technol.* 9, 8497–8506. doi:10.1016/j.jmrt.2020.05.122

Swiler, D. R., Detrie, T. J., and Axtell, E. A. (2003). *Rare Earth Transition Metal Oxide Pigments*. US, US6582814 B2.

Wu, Y., Qiu, K., Tang, Q., Zhang, W., and Wang, J. (2018). Luminescence Enhancement of Al^{3+} Co-doped $Ca_3Sr_3(VO_4)_4$:Eu^{3+} Red-Emitting Phosphors for White LEDs. *Ceram. Int.* 44, 8190–8195. doi:10.1016/j.ceramint.2018.01.267

Yang, R., Han, A., Ye, M., Chen, X., and Yuan, L. (2017). Synthesis, Characterization and Thermal Performance of Fe/N Co-doped $MgTiO_3$ as a Novel High Near-Infrared Reflective Pigment. *Sol. Energy Mater. Sol. Cells* 160, 307–318. doi:10.1016/j.solmat.2016.10.045

Yuan, L., Han, A., Ye, M., Chen, X., Yao, L., and Ding, C. (2018). Synthesis and Characterization of Environmentally Benign Inorganic Pigments with High NIR Reflectance: Lanthanum-Doped $BiFeO_3$. *Dyes Pigments* 148, 137–146. doi:10.1016/j.dyepig.2017.09.008

Zhang, S., Pan, Z., and Wang, Y. (2018). Synthesis and Characterization of (Ni, Sb)-Co-Doped Rutile Ceramic Pigment via Mechanical Activation-Assisted Solid-State Reaction. *Particuology* 41, 20–29. doi:10.1016/j.partic.2017.12.016

Zhao, X., Zhang, Y., Huang, Y., Gong, H., and Zhao, J. (2015). Synthesis and Characterization of Neodymium Doped Yttrium Molybdate High NIR Reflective Nano Pigments. *Dyes Pigments* 116, 119–123. doi:10.1016/j.dyepig.2015.01.018

Zhou, N., Sha, S., Zhang, Y., Li, S., Xu, S., and Luan, J. (2020). Coprecipitation Synthesis of a Green Co-doped Wurtzite Structure High Near-Infrared Reflective Pigments Using Ammonia as Precipitant. *J. Alloys Compd.* 820, 153183–483191. doi:10.1016/j.jallcom.2019.153183

Zou, J., and Zhang, P. (2020). Ni-doped BaTi5O11: New Brilliant Yellow Pigment with High NIR Reflectance as Solar Reflective Fillers. *Ceram. Int.* 46, 3490–3497. doi:10.1016/j.ceramint.2019.10.063

Conflict of Interest: The authors declare that the research was conducted in the absence of any commercial or financial relationships that could be construed as a potential conflict of interest.

Publisher's Note: All claims expressed in this article are solely those of the authors and do not necessarily represent those of their affiliated organizations, or those of the publisher, the editors and the reviewers. Any product that may be evaluated in this article, or claim that may be made by its manufacturer, is not guaranteed or endorsed by the publisher.